# Vibrationally Selected $O^+$-$O^+$ Fragmentation of $O_2$ below the Adiabatic Double-Ionization Potential Studied via Electron-Electron Coincidence Spectroscopy

P. Bolognesi,[1] D. B. Thompson,[1,*] L. Avaldi,[2] M. A. MacDonald,[3] M. C. A. Lopes,[1,†] D. R. Cooper,[1] and G. C. King[1]
[1]*Physics Department, The University of Manchester, M13 9PL Manchester, United Kingdom*
[2]*IMAI del CNR, Area della Ricerca di Roma, CP10-00016 Monterotondo, Italy*
[3]*Daresbury Laboratory, Daresbury, Warrington, WA4 4AD, United Kingdom*

(Received 5 October 1998)

Mechanisms for $O_2$ photofragmentation leading to the formation of the $O^+$-$O^+$ ion pairs, at photon energies below the adiabatic double-ionization threshold, have been investigated using a threshold-photoelectron-photoelectron coincidence technique. The selectivity and high efficiency of the experimental technique have allowed the process to be followed step by step. The measurements show that fast dissociation of a singly charged ion, followed by atomic autoionization, is the dominant decay route in this energy region. [S0031-9007(99)08566-X]

PACS numbers: 33.60.Cv, 33.80.Eh

For a diatomic molecule, the potential energy curve of the doubly charged positive ion (di-cation) is repulsive at large internuclear distances, although electron exchange interactions may result in a local minimum capable of supporting vibrational motion. Vibrational levels resulting from such a local minimum have been observed for di-cation ground states of several diatomic molecules [1–3]. In all of these cases, the adiabatic threshold for double photoionization is observed to lie above the lowest limit for dissociation into a pair of singly charged positive ion (cation) fragments. (Here, adiabatic double-ionization threshold refers to the minimum photon energy required for population of the $\nu = 0$ level of a molecule's di-cation ground state [4].) For some molecules, it is possible to produce a pair of cation fragments at photon energies below the adiabatic double-ionization (DI) threshold. These *below-threshold cation pairs* were first observed in ion-ion coincidence experiments on $H_2O$ [5] and CO [6].

The production of below-threshold cation pairs from a diatomic molecule involves the creation of a singly charged molecular ion whose potential curve crosses a di-cation curve in its repulsive part. Once created, the molecular ion may follow either of two alternative pathways. The first path involves a fast electronic decay that occurs as the molecular ion dissociates. Electrons released in this manner exhibit a broad, slowly varying energy distribution, depending on the internuclear distance at which the decay occurs [7]. The second path involves complete dissociation of the molecule to form an ion and an excited atomic fragment, which subsequently autoionizes. For this situation, the released electrons will have narrow energy distributions that are characteristic of atomic autoionization.

Creation of cation pairs via the two-step reaction paths described above may also occur at photon energies above the DI threshold of a molecule, but with additional competition from other dissociative double-ionization reactions, including direct double ionization. If below-threshold cation pairs can be produced from a given molecular species [5,6,8], it offers a unique opportunity to isolate the indirect reaction paths and study their competition. Such a study also investigates the competition between two time scales: the time scale of intramolecular electronic relaxation versus that of molecular dissociation. Conventional wisdom dictates that electronic relaxation is faster than dissociation. However, several experimental studies [9–12] have found instances in which molecular dissociation precedes electronic decay.

We have applied the threshold-photoelectron-photoelectron coincidence (TPEPECO) technique to study the dynamics of $O^+$-$O^+$ and $O_2{}^{2+}$ creation near its DI threshold. The study includes the measurement of TPEPECO spectra of $O_2$ collected at photon energies, where coincidence signals must originate from below-threshold $O^+$-$O^+$ formation. Production of below-threshold cation pairs from $O_2$ has not been observed previously. Moreover, we have been able to identify, for the first time, a vibrationally selective path for this reaction. The $O_2{}^{2+}$ $X\ {}^1\Sigma_g{}^+$ ground state is known to contain a local minimum capable of supporting 19 vibrational levels [3,13]. Hall *et al.* [3], using a related electron-electron coincidence technique, first identified the $O_2{}^{2+}$ $X\ {}^1\Sigma_g{}^+$ vibrational progression and located the DI threshold (corresponding to excitation to the $\nu = 0$ level) at 36.13 eV.

The main elements of the apparatus include a tunable photon beam, an effusive gas beam, and an electron coincidence spectrometer consisting of two electron energy analyzers. The photon beam was provided by the Daresbury Laboratory Synchrotron Radiation Source via the toroidal grating monochromator of beam line 3.3. The coincidence spectrometer has been described in detail by Hall *et al.* [14]. In the TPEPECO measurements, one analyzer is operated in the "threshold mode," i.e., tuned to collect electrons with nearly zero kinetic energy, using the penetrating field technique [15]. The other analyzer is operated in the conventional way to detect electrons of finite kinetic energy. True coincidences between near-zero-energy and finite-energy electrons are measured via standard coincidence counting electronics.

The present study includes two types of TPEPECO measurements. In the first, the photon energy is held fixed and the collection energy of the conventional analyzer is scanned over a range of kinetic energy, giving "constant-photon-energy spectra." In the second type, giving "constant-kinetic-energy spectra," the collection energy of the conventional analyzer is held fixed, while the photon energy is scanned over the region of interest. The presence of the same electron pairs in both types of measured spectra and a measurement of the incident photon flux via an $Al_2O_3$ diode establish a common relative scale of coincidence yield among all of the measurements.

The study also includes measurement of the noncoincidence yield of near-zero-energy electrons, collected simultaneously with each constant-kinetic-energy TPEPECO spectrum. This forms a threshold photoelectron (TPE) spectrum which maps out all single ion states created with the ejection of a near-zero-energy electron. Then, a constant-kinetic-energy TPEPECO spectrum covering photon energies below the DI threshold will select out single ion states that are precursors to electronic decay. Vice versa, in a constant-photon-energy TPEPECO spectrum, the coincidence yield maps out all of the possible decay products of the ion state marked by the detection of the near-zero-energy electron.

A set of constant-photon-energy TPEPECO spectra is shown in Fig. 1. Photon energies were chosen to sample from the region from the lowest dissociation limit [$O^+$ ($^4S$) + $O^+$ ($^4S$)] at 32.35 eV through the [$O^+$ ($^2D$) + $O^+$ ($^2D$)] dissociation limit at 39.002 eV. In all of these spectra, a dominant signal is observed for coincidences between near-zero-energy electrons and electrons with kinetic energies of about 0.45 eV. At the highest photon energy, a nonvanishing coincidence yield is also observed between near-zero-energy electrons and electrons with kinetic energies of about 0.8 eV. Coincidences due to the direct formation of the $O_2{}^{2+}$ $X$ state are expected to appear in the spectrum collected at $h\nu = 37.91$ eV, according to the measured DI threshold [3] and the Franck-Condon distribution of about 2 eV. However, no trace of the vibrational progression associated with the $O_2{}^{2+}$ $X$ state can be discerned in the spectrum.

In the spectra of Fig. 1, the production of electrons with the same well-defined kinetic energy at all of the photon energies investigated indicates that the dominant mechanism for double ionization is a two-step reaction. Moreover, we interpret the observed coincidence yield in these spectra as a clear indication of atomic autoionization. The two-step reaction occurs after the photon creates an $O_2{}^{+*}$ excited ion and a near-zero-energy electron. The precursor ion then dissociates into a singly charged oxygen ion and an excited $O^*$ ($2p^3$ $^2P$,$^2D$ $nl$) neutral fragment. The fragment is embedded in the $O^+$ ($^4S$) continuum and autoionizes via emission of an electron with kinetic energy between 0.4 and 2 eV [10]. The autoionizing decays $O^*$ ($2p^3$ $^2D$ $3p$) $^1P$,$^3D$ $\rightarrow$ $O^+$ ($^4S$) and $O^*$ ($2p^3$ $^2P$ $3s$) $^3P$ $\rightarrow$ $O^+$ ($^4S$) give rise to electrons with energy distributions peaking at 0.42 and 0.49 eV, respectively, while the autoionizing decays $O^*$ ($2p^3$ $^2P$ $3s$) $^1P$ $\rightarrow$ $O^+$ ($^4S$) and $O^*$ ($2p^3$ $^2D$ $3p$) $^1D$ $\rightarrow$ $O^+$ ($^4S$) give rise to electrons with a distribution that peaks at 0.8 eV [10]. This interpretation is consistent with one by Price and Eland [16] of their electron-electron coincidence spectra obtained using radiation from a He II lamp. With the identification of the two-step reaction, the question to be addressed is what precursor ion states are involved.

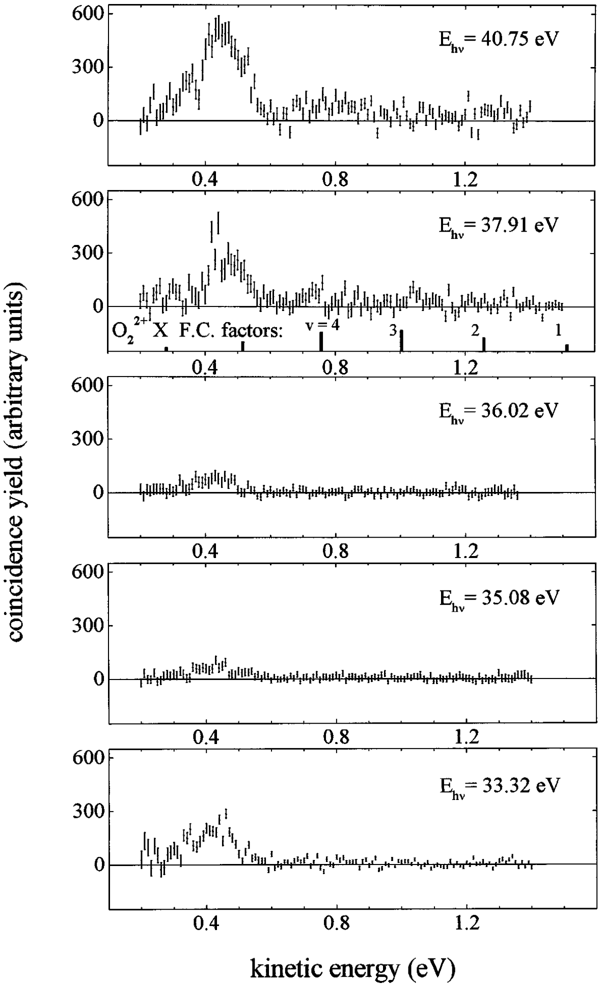

FIG. 1. $O_2$ TPEPECO spectra collected at five constant photon energies, below and above the adiabatic double ionization threshold (DIP = 36.13 eV). The solid bars in the spectrum at $E_{h\nu} = 39.71$ eV mark the energy positions and the Franck-Condon factors of the vibrational levels of the $O_2{}^{2+}$ ground state [3]. Resolution in these spectra is limited by the resolution of the conventional analyzer, which was 80 meV.

To examine the precursor ion states, we fixed the kinetic energy of the photoelectron at $E_k = 0.45$, 0.6, and 0.8 eV, respectively, and scanned the coincidence yield over the photon energy range between 32.5 and 41 eV. Of the three resultant constant-kinetic-energy TPEPECO spectra, the coincidence yield below the DI threshold is appreciable only for the spectrum collected with $E_k = 0.45$ eV, especially in the region around 33 eV (Fig. 2). Practically no signal is detected in the spectrum collected with $E_k = 0.6$ eV, and, for $E_k = 0.8$ eV, a nonvanishing signal occurs only at photon energies above the $O_2{}^{2+}$ $X$ state. Hence, we collected a second constant kinetic energy TPEPECO spectrum with $E_k = 0.45$, covering the region around 33 eV but at a higher photon resolution (Fig. 3). The TPE spectrum shows a broad feature likely due to vibrational components of several $O_2{}^+$ states. TPE spectra reported previously by Ellis *et al.* [17] and Tanaka *et al.* [18], as well as photoelectron spectra [19] and $(e, 2e)$ measurements [20], locate in this region a $^2\Pi_u$ valence ion state and lower members of the $(ns\sigma)$ and $(nd\sigma)$ $^2\Sigma_g$ Rydberg ion states, where $n = 4$ and 3, respectively. To simplify the understanding of Fig. 3, only markers indicating energy positions of the $^2\Pi_u$ vibrational levels are shown. However, all of the peak structures in the TPE spectrum can be uniquely assigned to vibrational levels of these three states. It is evident from Fig. 3 that the two peaks appearing in the coincidence yield align with the $^2\Pi_u$ $\nu = 5$ and 6 levels. To identify these $O_2{}^+$ $^2\Pi_u$ levels as precursor states, the complete reaction path that produces the dissociation into the $O^+ + O^*$ fragments has to be unraveled.

The model we propose involves predissociation of the $^2\Pi_u$ state via a Rydberg state that fragments into $O^+$ $(^4S)$ + $O^*$ $(^2P, {}^2D\ 3p$ or $3s)$. The Rydberg state has to belong to one of the series converging to the $O_2{}^{2+}$ $B$ or higher lying states. Because both the $O_2{}^{2+}$ $X$ and $A$ states have a dissociation limit corresponding to $O^+$ $(^4S)$ + $O^+$ $(^4S)$, Rydberg series converging to these states will never produce an excited fragment that autoionizes to $O^+$ $(^4S)$. A selection rule for the crossing of the potential curves limits the search for the predissociating state to those with ungerade symmetry [21]. This rule holds in all of the possible coupling schemes for the $O_2{}^{+*}$ states. We have produced potential curves for Rydberg $O_2{}^+$ states, using $O_2{}^{2+}$ potential curves obtained from complete-active-space self-consistent-field calculations [13], and using the Rydberg formula with reported $ns$ and $np$ quantum defects [22]. Assuming that the Rydberg ion states must have ungerade symmetry, and that the shapes of their potential curves parallel those of the corresponding di-cation states (at least over the spatial range spanned by the $^2\Pi_u$ state's potential minimum), we have produced potential curves for the $O_2{}^{+*}$ $(B\,^3\Pi_g + np\sigma)$, $(B\,^3\Pi_g + np\pi)$, $(B\,^3\Sigma_u{}^- + ns\sigma)$, and $(W\,^3\Delta_u + ns\sigma)$ Rydberg series.

The energy region where the different curves occur limits the possible Rydberg ion states to $(B\,^3\Pi_g + 3p\sigma)$, $(B\,^3\Pi_g + 3p\pi)$, $(B\,^3\Sigma_u{}^- + 3s\sigma)$, and $(W\,^3\Delta_u + 3s\sigma)$. Considering that the last state has $O^+$ $(^4S)$ + $O^*$ $(^2D\ 3s)$ as a dissociation limit and thus the autoionizing electron would not be detectable in the present experiment, we are left with only three states. The calculated potential curves for these states are shown in Fig. 4 together with the $^2\Pi_u$ potential curve, calculated using a Morse potential with the $\omega_e$ and $\omega_e x_e$ given by Tanaka *et al.* [18]. The only adjustable parameter used here is the equilibrium internuclear distance for the $^2\Pi_u$ state. The value chosen is 1.3 Å which compares with the value of 1.2 Å for the ground state of neutral oxygen [21]. The configuration describing the $^2\Pi_u$ state is formed from that of the neutral ground state by removal of a $2p\pi_u$ bonding electron [23], and the equilibrium distance chosen for the $^2\Pi_u$ state is consistent with a transition from a bonding to an antibonding orbital. The chosen value is also quite similar to those given for lower $O_2{}^+$ states [21] formed by removal of an electron from a $2p\pi_u$ orbital.

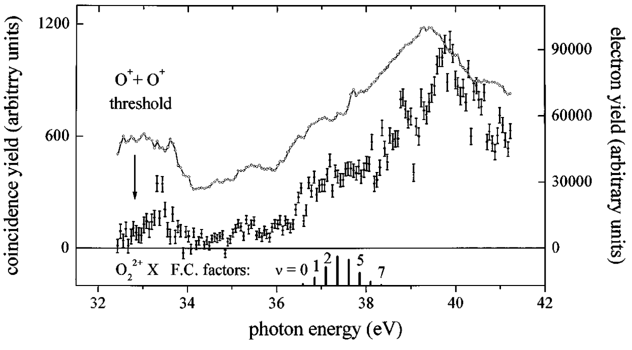

FIG. 2. A 0.45 eV constant kinetic energy TPEPECO (|) spectrum together with the corresponding TPE (—) spectrum. The photon energy range extends from the lowest $O^+$-$O^+$ dissociation limit through the $O_2{}^{2+}$ ground state. The solid bars mark the energy positions and Franck-Condon factors of the vibrational levels of the $O_2{}^{2+}$ ground state [3]. Resolution in both the TPEPECO and TPE spectra are limited by the photon bandpass, which was set at 120 meV.

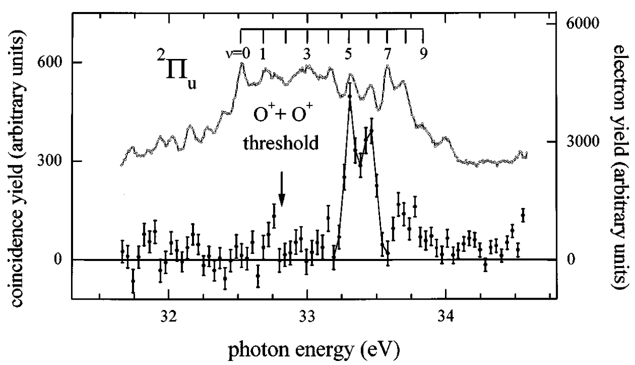

FIG. 3. A 0.45 eV constant kinetic energy TPEPECO (|) spectrum together with the corresponding TPE (—) spectrum over the photon energy range just above the lowest $O^+$-$O^+$ dissociation limit. The positions of vibrational levels of the $O^+$ $^2\Pi_u$ state are indicated. The photon bandpass was set at 80 meV.

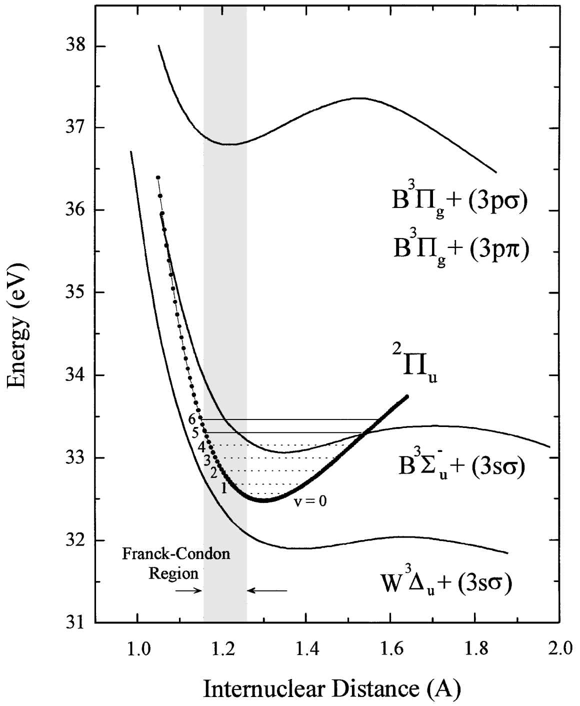

FIG. 4. Potential energy curves of $O_2^+$ states with ungerade symmetry in the region of the double-ionization threshold. The $O_2^+$ $^2\Pi_u$ state curve is calculated from experimental parameters given by Ref. [18], as described in the text. The $O_2^+$ Rydberg states were calculated using theoretical $O_2^{2+}$ potential curves [13] and experimental quantum defects [22].

Despite the simplicity of the model used, Fig. 4 shows that the $O_2^+$ $(B\,^3\Sigma_u^- + 3s\sigma)$ Rydberg state crosses the $^2\Pi_u$ state exactly in the region where the coincidence yield has been observed. Thus, the crossing allows the $\nu = 5, 6$ levels of the $^2\Pi_u$ state to be predissociated by the $(B\,^3\Sigma_u^- + 3s\sigma)$ Rydberg state, which then dissociates into $O^+$ $(^4S)$ + $O^*$ $(^2P\ 3s)$. Further support for the proposed model comes from the observation that the $^2\Pi_u$ and the $(B\,^3\Sigma_u^- + 3s\sigma)$ state have configurations that differ only by the location of the outermost electron. In Fig. 4, the $(B\,^3\Sigma_u^- + 3s\sigma)$ and $^2\Pi_u$ potential curves cross again in the innerwell region above 35 eV. Thus, the model predicts that a coincidence yield may also appear above this value. Indeed, inspection of the TPEPECO spectrum in Fig. 2 shows that, below the DI threshold, the only other significant structure in the coincidence yield does appear in the region above 35 eV. Remarkably then, the model shows that all production of below-threshold cation pairs from $O_2$ can be associated with creation of a single precursor ion state.

The high selectivity and efficiency of the TPEPECO technique demonstrate that fast dissociation of a molecular ion followed by atomic autoionization is the dominant process leading to the production of $O^+$-$O^+$ ion pairs in the vicinity of the adiabatic double-ionization threshold. Analysis of the TPEPECO spectra (i) finds that, below this threshold, only this one reaction path leads to the formation of cation pairs and (ii) shows the reaction is vibrationally selective. Applying a simple model, we have identified a single precursor ion state that is the likely candidate responsible for the production of all below-threshold cation pairs.

The authors thank D. Edvardsson for providing the potential energy curves of $O_2^{2+}$ and Nguyen Xuan Chieu for useful discussions. One of us (M. C. A. Lopes) gratefully acknowledges the support from CAPES. This work was partially supported by the NATO C.R.G. 960141.

---

[*] Present address: Chemistry Department, State University of New York, Stony Brook, NY 11794-3400.

[†] Present address: Departamento de Fisica, ICE, Universidade Federal de Juiz de Fora, MG, CEP:36036-330, Brazil.

[1] A. G. McConkey *et al.,* J. Phys. B **27**, 271 (1994).
[2] G. Dawber *et al.,* J. Phys. B **27**, 2191 (1994).
[3] R. I. Hall *et al.,* Phys. Rev. Lett. **68**, 2751 (1992).
[4] J. H. D. Eland, *Photoelectron Spectroscopy* (Butterworths, London, 1984), 2nd ed.
[5] D. Winkoun, G. Dujardin, L. Hellner, and M. J. Besnard, J. Phys. B **21**, 1385 (1988).
[6] P. Lablanquie *et al.,* Phys. Rev. A **40**, 5673 (1989).
[7] U. Becker *et al.,* Phys. Rev. A **45**, R1295 (1992).
[8] J. H. D. Eland *et al.,* J. Phys. B **30**, 2177 (1997).
[9] P. Morin and I. Nenner, Phys. Rev. Lett. **56**, 1913 (1986).
[10] A. A. Wills, A. A. Cafolla, and J. Comer, J. Phys. B **24**, 3989 (1991); A. A. Cafolla, T. Reddish, and J. Comer, J. Phys. B **22**, L273 (1989).
[11] A. V. Golovin *et al.,* Phys. Rev. Lett. **79**, 4554 (1997).
[12] D. B. Thompson *et al.,* J. Phys. B **30**, L147 (1997).
[13] M. Lundqvist *et al.,* J. Phys. B **75**, 499 (1996).
[14] R. I. Hall *et al.,* Meas. Sci. Technol. **3**, 316 (1992).
[15] S. Cvejanovic and F. H. Read, J. Phys. B **7**, 1180 (1974).
[16] S. D. Price and J. H. D. Eland, J. Phys. B **24**, 4379 (1991).
[17] K. Ellis *et al.,* J. Phys. B **27**, 3415 (1994).
[18] T. Tanaka *et al.,* J. Electron Spectrosc. Relat. Phenom. **79**, 507 (1996).
[19] J. H. D. Eland and E. J. Duerr, Chem. Phys. **229**, 1 (1998).
[20] C. E. Brion, K. H. Tan, M. J. van der Weil, and P. E. van der Leeuw, J. Electron Spectrosc. Relat. Phenom. **17**, 101 (1979).
[21] G. Herzberg, *Molecular Spectra and Molecular Structure I. Spectra of Diatomic Molecules* (Van Nostrand, New York, 1950).
[22] B. A. van der Kamp, R. S. Hiemstra, and W. J. van der Zande, J. Chem. Phys. **99**, 7487 (1993).
[23] A. Gerwer, C. Asaro, B. V. McKoy, and P. W. Langhoff, J. Chem. Phys. **72**, 713 (1980).